Structural Engineering and Mechanics, *Vol. 49, No. 2 (2014) 203-223*
DOI: http://dx.doi.org/10.12989/sem.2014.49.2.203

Vehicle-bridge coupling vibration analysis based fatigue reliability prediction of prestressed concrete highway bridges

Jinsong Zhu[1,2a], Cheng Chen[2b] and Qinghua Han[*3]

[1]*Key Laboratory of Coast Civil Structure Safety, Ministry of Education, Tianjin University, Tianjin 300072, People's Republic of China*
[2]*School of Engineering, San Francisco State University, San Francisco, CA 94132, USA*
[3]*School of Civil Engineering, Tianjin University, Tianjin 300072, People's Republic of China*

(Received June 17, 2013, Revised October 21, 2013, Accepted December 9, 2013)

Abstract. The extensive use of prestressed reinforced concrete (PSC) highway bridges in marine environment drastically increases the sensitivity to both fatigue- and corrosion-induced damage of their critical structural components during their service lives. Within this scenario, an integrated method that is capable of evaluating the fatigue reliability, identifying a condition-based maintenance, and predicting the remaining service life of its critical components is therefore needed. To accomplish this goal, a procedure for fatigue reliability prediction of PSC highway bridges is proposed in the present study. Vehicle-bridge coupling vibration analysis is performed for obtaining the equivalent moment ranges of critical section of bridges under typical fatigue truck models. Three-dimensional nonlinear mathematical models of fatigue trucks are simplified as an eleven-degree-of-freedom system. Road surface roughness is simulated as zero-mean stationary Gaussian random processes using the trigonometric series method. The time-dependent stress-concentration factors of reinforcing bars and prestressing tendons are accounted for more accurate stress ranges determination. The limit state functions are constructed according to the Miner's linear damage rule, the time-dependent *S-N* curves of prestressing tendons and the site-specific stress cycle prediction. The effectiveness of the methodology framework is demonstrated to a *T*-type simple supported multi-girder bridge for fatigue reliability evaluation.

Keywords: corrosion-fatigue; vehicle-bridge coupling vibration; reliability assessment; prestressed reinforced concrete bridge

1. Introduction

Due to the fact that structures are becoming more slender, the traffic volume is increasing, the axial loads are larger, and the traffic speed limits are higher, research interest on fatigue in concrete structures has increased in the past few years (Stangenberg *et al.* 2009). Concrete fatigue is mainly a problem of offshore structures, railway sleepers and bridges because these types of structures are often exposed to repeated loading. With increased axial loads the condition for the bridges has

∗Corresponding author, Professor, E-mail: qhhan@tju.edu.cn
[a]Professor, Visiting Research Scientist
[b]Assistant Professor

http://www.techno-press.org/?journal=sem&subpage=8 ISSN: 1225-4568 (Print), 1598-6217 (Online)

changed and many existing bridges are nowadays required to carry larger loads than that they originally designed for. In addition, the extensive use of bridges in marine environment drastically increases the sensitivity to both fatigue- and corrosion-induced damage of their critical structural components during their service lives (Emilio *et al.* 2009). A girder in the fully prestressed or uncracked condition is very resistant to fatigue failure (Warner and Hulsbos 1966, Rigon and Thürlimann 1985), owing to the limited stress range occurring in prestressing tendons. But if the girder cracks due to overload, the local stress concentration of prestressing tendons nearby cracks and accelerated corrosion degeneration will increase the risk of fatigue failure of prestressed reinforced concrete (PSC) bridges. However, very limited studies exist for performance prediction of PSC highway bridges under coupled corrosion-fatigue action to the best knowledge of the authors.

Structural reliability analysis has been widely applied in many fields. Reliability theory is concerned with the probabilistic measure of safe performance. For fatigue reliability, both resistance (capacity) and load effect (demand) have to be evaluated. Generally, a larger amount of uncertainty is involved in fatigue evaluations compared with bridge strength evaluations or load ratings. Furthermore, the demand for a realistic fatigue evaluation is much higher than that for a fatigue design, since an over-conservative evaluation result could cost considerably more than an over-conservative design. An un-conservative result is, of course, not desired either. Besides the uncertainty factors mentioned above, there are also other sources of uncertainty in the fatigue evaluation process. These include the scatter nature of the S-N curves, variable truck loads including significant site-to-site variations, approximations in structural analysis or load effect estimation, and etc. The inherent uncertainties, however, can be reduced using more refined analyses or field measurements to better define the stress range at the details under investigation.

As indicated above, the fatigue performances of PSC highway bridges should be described in the context of reliability theory. Certainly, there are many valuable efforts on the fields. A comprehensive reference work on the existing fatigue reliability approaches for reassessment of steel structures, including railway and highway bridges, can be found in Byers *et al.* (1997). Guo and Chen (2011) evaluated the fatigue reliability of retrofitted steel bridge details based on the field stress and displacement measurements. Kwon and Frangopol (2010) presented a fatigue reliability assessment method of steel bridges using probability density functions of equivalent stress range based on field monitoring data. Wu *et al.* (2012) developed a reliability based fatigue assessment model, which can rationally consider the combined load effects from wind and traffic. In their framework, the monitoring data during service life is the most necessary information. The model thus does not apply to newly constructed bridges or bridges lack of the monitoring responses in the fatigue-prone details. Urgent needs therefore exist for a numerical method to track the fatigue reliability evolvement of any bridge. Pipinato and Modena (2010) performed a fatigue reliability assessment analysis of an old steel arch bridge along with traffic estimation for various scenarios in order to derive a reasonable assessment of remaining fatigue life. More recently，Zhang and Cai (2012) presented a framework of fatigue reliability assessment for existing steel bridges in lifetime serviceability. The effects of road surface condition, vehicle speed, and annual traffic increase rate are investigated for the fatigue reliability index and fatigue life. The vehicle-bridge coupled vibration analysis was used to obtain more actual stress history of critical location by including the impact effect of vehicle load automatically.

Nevertheless, most of these researches on reliability-based analysis of fatigue have focused on steel and composite bridges. Very limited work has been done on the fatigue performance study of PSC bridges. Cesar and Joan (1998) presented an analysis model for fatigue reliability of

prestressed concrete bridges. Petryna *et al.* (2002) presented a computational framework for fatigue reliability analysis of reinforced concrete structures. According to their work, the localization effect of corrosion and crack on embedded steel bars, the multiple presence factors of vehicles on different lanes, and degeneration of fatigue properties of prestressing tendons due to corrosion, etc. should be taken into consideration for the fatigue reliability prediction of PSC bridges. There exist needs for more work on fatigue reliability and remaining fatigue life prediction of PSC bridges.

The motivation of this paper is to integrate previous researches on corrosion and fatigue to develop a probability framework for fatigue reliability evaluation of PSC highway bridges. The time-dependent stress-concentration factors of reinforcing bar and prestressing tendons are taken into consideration for more accurate stress ranges determination. Three-dimensional nonlinear mathematical models of typical fatigue trucks are developed. Road surface roughness is simulated as transversely correlated random processes. The multi-girder bridges are treated as a grillage beam system. Fatigue damage analysis and fatigue reliability assessment is performed according to the Miner's linear damage rule, the time-dependent *S-N* curves of prestressing tendons and the site-specific stress cycles. A T-type simple supported multi-girder bridge is taken the example for illustrating the methodology framework for fatigue reliability evaluation of PSC highway bridges.

The method of vehicle-bridge coupling vibration analysis is described in Section 2. Section 3 presents a revised strategy for equivalent stress range of the steel bars or prestressing tendons taking into account the multiple presence factor and the stress-concentration factor. The flowchart of the present fatigue reliability prediction is summarized in Section 4. Finally, an application to a PSC bridge is given in Section 5.

2. Vehicle-bridge coupling vibration system

2.1 Vehicle and bridge model

Most of the previous analytical studies were focused on the vehicle-bridge coupling vibration analysis for obtaining the dynamic response of bridges under vehicle-induced vibration. Wang *et al.* (1992), Huang *et al.* (1993) developed a three-dimensional nonlinear truck model for the American Association of State Highway and Transportation Officials (AASHTO 2007) standard design truck HS20-44, which also is used in the present study to represent the trucks with three axles. The truck is simplified as three-dimensional nonlinear truck model (see as Fig. 1). This model can also be used to represent other simpler vehicles through defining the number and dimensions for each rigid body, mass block, and spring-damping system. A nonlinear spring and damp system is adapted to simulate the suspension system and the interaction between vehicles and structures. There are eleven independent degrees of freedom, which are expressed as vector:

$$\mathbf{Y}_V = \begin{bmatrix} y_{w1} & y_{w2} & y_{w3} & y_{w4} & y_{w5} & y_{w6} & y_{c1} & y_{c2} & \theta_{c1} & \varphi_{c1} & \varphi_{c2} \end{bmatrix}^T \tag{1}$$

where y_{w1}, y_{w2}, y_{w3}, y_{w4}, y_{w5} and y_{w6} are vertical displacements of six wheels, respectively; y_{c1} and y_{c2} are vertical displacements of the head and body of vehicle; θ_{c1} is the pitching displacement of the head of vehicle; φ_{c1} and φ_{c2} denote the lateral rolling displacements of the head and body of vehicle.

The dynamic model of bridges can be obtained through the finite-element method using beam,

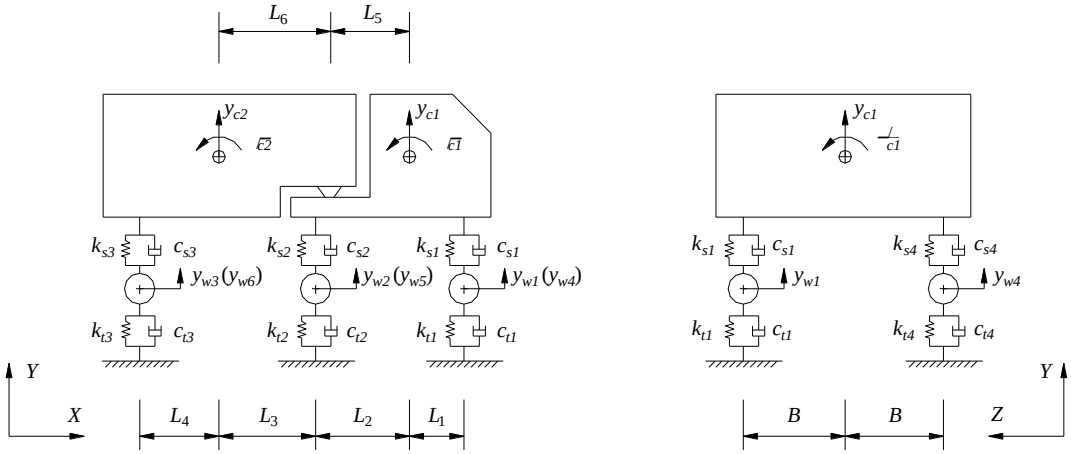

(a) Side view (b) Front view

Fig. 1 Model of three-axles vehicles

Table 1 Major parameters of vehicle (3 axles)

	Parameters	Values	Parameters	Values
Mass	m_{w1}(kg)	490	m_{w4}(kg)	490
	m_{w2}(kg)	808	m_{w5}(kg)	808
	m_{w3}(kg)	653	m_{w6}(kg)	653
Moment of inertia	I_{c1}(kg·m^2)	2022	J_{c1}(kg·m^2)	8544
	I_{c2}(kg·m^2)	33153	J_{c2}(kg·m^2)	181216
Spring stiffen	$ks1$(N/m)	242604	k_{t1}(N/m)	875082
	$ks2$(N/m)	1903172	k_{t2}(N/m)	3503307
	$ks3$(N/m)	1969034	k_{t3}(N/m)	3507429
	$ks4$(N/m)	242604	k_{t4}(N/m)	875082
	$ks5$(N/m)	1903172	k_{t5}(N/m)	3503307
	$ks6$(N/m)	1969034	k_{t6}(N/m)	3507429
Damping coefficient	c_{s1}(N·s/m)	2190	c_{t1}(N·s/m)	2000
	c_{s2}(N·s/m)	7882	c_{t2}(N·s/m)	2000
	c_{s3}(N·s/m)	7182	c_{t3}(N·s/m)	2000
	c_{s4}(N·s/m)	2190	c_{t4}(N·s/m)	2000
	c_{s5}(N·s/m)	7882	c_{t5}(N·s/m)	2000
	c_{s6}(N·s/m)	7182	c_{t6}(N·s/m)	2000
Length	L_1(m)	1.698	L_4(m)	2.283
	L_2(m)	2.569	L_5(m)	2.215
	L_3(m)	1.984	L_6(m)	2.338
	B(m)	1.1		

solid, or shell elements. The motion of the vehicle can be stated as the following equation according to D'Alembert principle

$$\boldsymbol{M}_V\ddot{\boldsymbol{Y}}_V + \boldsymbol{C}_V\dot{\boldsymbol{Y}}_V + \boldsymbol{K}_V\boldsymbol{Y}_V = \boldsymbol{F}_V \tag{2}$$

where, $\boldsymbol{M_V}$, $\boldsymbol{C_V}$ and $\boldsymbol{K_V}$ are the mass matrix, damping matrix, and stiffness matrix of the bridge, respectively; $\boldsymbol{F_V}$ is wheel-bridge contact forces on the bridge; and $\ddot{\boldsymbol{Y}}_{\boldsymbol{V}}$, $\dot{\boldsymbol{Y}}_{\boldsymbol{V}}$ and $\boldsymbol{Y_V}$ are acceleration, speed and displacement responses of the bridge, respectively. The geometry, mass distribution, damping, and stiffness of the tires and suspension systems of this truck are listed in Table 1.

2.2 Roadway profile

The roadway profile is usually assumed to be a zero-mean stationary Gaussian random process and can be generated through trigonometric series method based on a power spectral density function such as (Au *et al.* 2001)

$$r(x) = \sum_{k=1}^{N} \alpha_k \cos(2\pi\omega_k x + \theta_k) \tag{3}$$

$$\alpha_k{}^2 = 4S(\omega_k)\Delta\omega \tag{4}$$

$$\omega_k = \omega_l + (k - \frac{1}{2})\Delta\omega \tag{5}$$

$$\Delta\omega = (\omega_u - \omega_l)/N \tag{6}$$

where k is integer number; α_k is the amplitude of the cosine wave; θ_k is the random phase angle with uniform probability distribution in the interval [0, 2 π]; x is the global coordinate measured from the left end of the bridge; N is the total number of terms used to build up the road surface roughness and ω_k is the frequency within the interval [ω_l, ω_u]. In the interval [ω_l, ω_u], the power spectral density function $S(\omega_k)$ is defined as (Honda *et al.* 1982)

$$S(\omega_k) = \alpha_t \omega_k{}^{-\beta}, \omega_l < \omega_k < \omega_u \tag{7}$$

where the parameter α_t is a spectral roughness coefficient according to ISO 8608 (1995) and the exponent, β, is assumed to be 1.94.

In general, the roadway profile is degenerated in 15-year period and will be retrofitted, not only the fast lanes but also the slow lanes (Zhang and Cai 2012). The roadway profile in the first 10 years was classified as very good, the eleventh and twelfth years as good, the thirteenth year as average, and the fourteenth and fifteenth years as poor

$$\alpha_t = \begin{cases} \leq 0.12\times10^{-6} & t \leq 5 years \\ 0.12\times10^{-6} < \alpha_t \leq 1.0\times10^{-6} & t \leq 10 years \\ 0.24\times10^{-6} < \alpha_t \leq 1.0\times10^{-6} & 11 < t \leq 12 years \\ 1.0\times10^{-6} < \alpha_t \leq 4\times10^{-6} & 12 < t \leq 13 years \\ 4\times10^{-6} < \alpha_t \leq 16\times10^{-6} & 13 < t \leq 14 years \\ 16\times10^{-6} < \alpha_t \leq 50\times10^{-6} & 14 < t \leq 15 years \end{cases} \tag{8}$$

2.3 Analysis of vehicle-bridge coupling vibration

The equations of motion for a bridge under external loads can be written as follows

$$\boldsymbol{M_B}\ddot{\boldsymbol{Y}}_{\boldsymbol{B}} + \boldsymbol{C_B}\dot{\boldsymbol{Y}}_{\boldsymbol{B}} + \boldsymbol{K_B}\boldsymbol{Y}_B = \boldsymbol{F_B} \tag{9}$$

where $\ddot{\boldsymbol{Y}}_{\boldsymbol{B}}$, $\dot{\boldsymbol{Y}}_{\boldsymbol{B}}$ and $\boldsymbol{Y_B}$ denote bridge acceleration, velocity and displacement vectors, respectively; $\boldsymbol{M_B}$, $\boldsymbol{C_B}$ and $\boldsymbol{K_B}$ represent general mass, damping and stiffness matrices of bridge, respectively; $\boldsymbol{F_B}$ is the vector of the forces acting on the bridge.

The structure damping is assumed as Rayleigh damping (Leitão *et al.* 2011) and expressed by mass and stiffness matrix as

$$\boldsymbol{C_B} = \alpha_0 \boldsymbol{M_B} + \beta_0 \boldsymbol{K_B} \tag{10}$$

The parameters α_0 and β_0 are computed, respectively, by

$$\beta_0 = \frac{2(\xi_2\omega_{02} - \xi_1\omega_{01})}{\omega_{02}\omega_{02} - \omega_{01}\omega_{01}} \tag{11}$$

$$\alpha_0 = 2\xi_1\omega_{01} - \beta_0\omega_{01}\omega_{01} \tag{12}$$

where ω_{01} and ω_{02} are the first and second natural frequencies of structure; ξ_1 and ξ_2 are the first and second modal damping ratio of structure.

Assuming that wheels always cling to the deck when vehicle moving through bridge, the interaction forces between wheels and bridge can be expressed as

$$f_i(t) = k_i\Delta_i(t) + c_i\dot{\Delta}_i(t) \tag{13}$$

where the subscript i denotes the i^{th} wheel; k_i and c_i is stiffness coefficient and damp coefficient, for the tyre of the i^{th} wheel, respectively; $\Delta_i(t)$ is the vertical displacement of the i^{th} wheel relative to the deck at time instant t, as shown

$$\Delta_i(t) = y_i(t) - z_i(t) - r_i \tag{14}$$

where $y_i(t)$ is the vertical displacement of the i^{th} wheel at time t; $z_i(t)$ is the vertical displacement of bridge in the position where the i^{th} wheel contact the bridge at time t and r_i is the irregularity function value in the position where the i^{th} wheel contact the bridge.

According to the condition of displacement and force compatibility between vehicle and bridge, the vibration equations of vehicle model and bridge model are coupled. The mass matrix, stiffness matrix, and damping matrix of the bridge in this study are obtained from ANSYS® finite element analysis and the corresponding matrices of vehicles are automatically assembled in the MATLAB environment using the fully computerized approach. A Newmark-β algorithm based professional procedure is developed in MATLAB® version R2009a to solve this coupled and time-varying second-order ordinary differential equations and the dynamic responses of vehicle and bridge can be derived (Zhu and Yi 2013).

3. Equivalent stress range

3.1 Sectional stress analysis

A modular ratio is needed to calculate the neutral axis, moment of inertia and finally the stresses in a section. This ratio, which will be referred to as α_{sc} hereafter, determines the distribution of stresses between the concrete and the reinforcing or prestressing steel.

The α_{sc} is calculated with regard to the Young's modulus of the materials

$$\alpha_{sc} = E_{s(p)} / E_c \tag{15}$$

where $E_{s(p)}$ is the characteristic modulus of elasticity for reinforcing steel or prestressing tendons, which is denoted by the suffix *s* or *p*, respectively; E_c is the mean modulus of elasticity for concrete.

With the assumption that the steel and concrete have full interaction, the Navier's formula can be used to calculate the stresses in the effective transformed concrete section. The stress of reinforcing steel or prestressing steel due to the traffic load can then be calculated as

$$\sigma_{s(p)} = \alpha_{s(p)} \cdot \frac{M}{I_{ef}} \cdot z \tag{16}$$

where M is the bending moment caused by the permanent load combined with the current traffic load; z is the sectional coordinate from the center of gravity; I_{ef} is the moment of inertia of the transformed concrete section.

3.2 Stress-concentration factors of steel bar

The stress-concentration factor affects the fatigue life of the reinforcing steel bars and thus the fatigue life of the reinforced concrete beams. Many factors affect the stress-concentration factor and include the geometry of the notch, material type, and especially the pit depth of corrosion. When the geometry of the notch and the mechanical properties are uniform, differences due to corrosion of the reinforcing steel bars will cause different stress-concentration factor in different service years.

After corrosion of steel bars initiates, it has been reported that cover and concrete quality affect corrosion rates. The corrosion rate may be predicted as a function of the concrete quality, cover, and time since corrosion initiation (Vu and Stewart 2000)

$$i_{corr}(1) = \frac{27(1 - W/C)^{-1.64}}{C_{cover}} \tag{17}$$

where $i_{corr}(1)$ is the corrosion rate at the start of corrosion propagation, which is given in μA/cm^2 (1μA/cm^2=0.0116 mm/year), *W/C* is the water/cement ratio, and C_{cover} is given in mm. Vu and Stewart (2000) suggested that corrosion rate can be expressed as a time dependent variable

$$i_{corr}(t) = 0.85 \cdot i_{corr}(1) \cdot t^{-0.29} \quad (t \geq 1 \text{ year}) \tag{18}$$

Thus, the depth of a pit, p (which is equivalent to the maximum penetration of pitting and is given in mm) after t years since corrosion initiation, i.e., $p(t)$, can be evaluated as

$$p(t) = 0.0116 i_{corr}(t) t \tag{19}$$

Based on the study by Al-Hammoud *et al.* (2011), a linear relationship between the mean value of stress-concentration factor of steel bars $\overline{\kappa}$ and pit depth of corrosion can be statistically presented as follows

$$\overline{\kappa} = 1.225 + 0.538 p(t) \tag{20}$$

Substituting Eq. (19) into Eq. (20) gives

$$\overline{\kappa} = 1.225 + 0.00624 \cdot i_{corr}(t) \cdot t \tag{21}$$

The stress-concentration factor of steel bars κ is assumed as normal distribution with mean value of $\overline{\kappa}$, coefficient of variation (COV) of 0.35, and truncated by 1.

3.3 Multiple presence factor

Truck loading is the primary cause of fatigue damage in PSC bridges. Heavy trucks may appear on a highway bridge span in one or more lanes simultaneously. Depending on structural configuration, trucks in multiple lanes can induce much higher load effects to bridge components than those in one lane. Therefore, the governing load effects due to these loading configurations need to be addressed for bridge evaluation.

Bowman *et al*. (2012) used Weigh-in-Motion data to derive the multiple presence factor (*MPF*). A large amount of WIM truck weight data was used to simulate and model the behavior of trucks and their load effects in bridge components. In general, longer spans allow more trucks to be simultaneously present on the span, higher truck traffic volumes increase the probability of such simultaneous presence, and more lanes available reduce such likelihood. The proposed *MPF* was thus given as a function of these three major causal factors: span length, ADTT, and number of lanes, which can be calculated by

$$MPF = 0.988 + 6.87 \times 10^{-5} \cdot L + 4.01 \times 10^{-6} \cdot [ADTT]_{PRESENT} + 1.07 \times 10^{-2} / n_L \geq 1 \tag{22}$$

where L is the span length in feet, $[ADTT]_{PRESENT}$ is the present average number of trucks per day for all directions of truck traffic including all lanes on the bridge, and n_L is the number of lanes.

The *MPF* in Eq. (22) simplifies the analysis for bridge design and evaluation by simply multiplying one lane load effect with n_L and *MPF* to obtain the total fatigue load effect (Bowman *et al*. 2012). It thus enables more reliable estimation of fatigue load effect, especially for fatigue evaluation of highway bridges for more reliable remaining life prediction.

3.4 Revised equivalent stress range

Due to one truck passage, the hot point stress history in critical section is tracked by vehicle-bridge coupling vibration analysis. The stress-range bin histogram data are collected by rain-flow counting method from the stress history due to one truck passage at the critical locations

of structural members. Since small cycles do not contribute to the overall fatigue damage, the rain-flow analysis algorithm can be programmed to ignore any stress ranges less than the stress range cut-off level. The stress range cut-off would influence the numbers of cycles per truck passage but would not influence the distribution of equivalent stress range and the fatigue reliability and fatigue life. The typically used threshold value 3.45 MPa is adopted herein for data analysis on the stress range obtained from field monitoring (Zhang and Cai 2012, Kwon and Frangopol 2010). The equivalent stress range S_{eq} is determined as

$$S_{eq} = \sum_{i=1}^{n} \left(\alpha_i \cdot S_{ri}^{m} \right)^{1/m} \tag{23}$$

where s_{ri} is the i^{th} stress-range bin in the stress-range bin; α_i is the occurrence frequency of the i^{th} stress-range bin; n is the total numbers of the stress-range bin histogram, and m is the material constant typically 3 (Byers *et al*. 1997).

The effects of multiple lanes presence and the stress-concentration on the equivalent stress range S_{eq} are revised as follows

$$S_{re} = n_L \cdot MPF \cdot \kappa \cdot S_{eq} \tag{24}$$

where S_{re} is the revised equivalent stress amplitude; n_L is the total numbers of lanes in the same transportation direction; κ is stress-concentration factor of steel bars.

4. Fatigue reliability assessment

4.1 Fatigue reliability analysis

The reliability of a structural component or system is generally related to the probability of not violating a particular limit-state. Based on the limit-state function (i.e., $g(\boldsymbol{X})=R-S$), the failure probability of a structural member is defined as $P_f=P(g(\boldsymbol{X})<0)$. The reliability index, β, that is related to the probability of failure can be defined as

$$\beta = \boldsymbol{\Phi}^{-1}\left(1 - P_f\right) = -\boldsymbol{\Phi}^{-1}\left(P_f\right) \tag{25}$$

where $\boldsymbol{\Phi}^{-1}(\cdot)$ denotes the inverse standard normal cumulative distribution function (CDF).

Fatigue life is critically dependent on stress ranges due to live load fluctuations from truck traffic. The fatigue resistance of prestressed beams is mainly controlled by the fatigue lives of prestressing tendons and reinforcement (Taly 1989, Collins and Mitchell 1987). Based on a fully probabilistic analysis of several bridge structures, Casas (1999) concludes that it is however not possible to draw general conclusions regarding whether reinforcing steels or prestressing tendons is governing fatigue safety.

The limit-state function used in fatigue reliability analysis is defined as follows

$$\mathrm{g}\left(\boldsymbol{X}\right) = \Delta - D(t) \tag{26}$$

where $D(t)$ is the accumulated damage at time t; Δ is the damage to cause failure and is treated as a random variable with a mean value of 1; and g is a failure function such that $g<0$ implies a fatigue failure.

The accumulated damage based on Miner's rule (Miner 1945) is

$$D(t)=\sum_i \frac{n_i}{N_i}=\frac{n_{tc}}{N_f} \tag{27}$$

where n_i is number of observations in the predefined stress-range bin S_{ri}; N_i is the number of cycles to failure corresponding to the predefined stress-range bin; n_{tc} is the total number of stress cycles, and N_f is the number of cycles to failure under an revised equivalent constant amplitude loading.

If the number of stress cycles due to the every truck passage is denoted as n_v, the cumulated number of truck passages for the future year t can be estimated as (Kwon and Frangopol 2010)

$$n_{tr}(t)=365\cdot n_v\cdot ADTT\cdot\int_0^t(1+\alpha)^t dt=365\cdot n_v\cdot ADTT\cdot\frac{(1+\alpha)^t-1}{\ln(1+\alpha)} \tag{28}$$

where t is the number of years, subscript tr means trucks only, and α is the traffic increase rate per year.

The total number of stress cycles in entire service life n_{tc} is

$$n_{tc}=\sum_{t=1}^{N_l} n_{tr}(t) \tag{29}$$

where N_l is the service life in year.

Due to corrosion of steel in service stage, the general S-N equation for steel is modified by the multiplication factor $\varphi(t)$ as follows (Li *et al.* 2009)

$$N=\varphi(t)\cdot A\cdot S_{re}^{-m} \tag{30}$$

where A is the detailed constant according to correlated test of the reinforcing steels or the prestressing tendons embedded in concrete, and $\varphi(t)$ indicates the deterioration factor due to corrosion. The statistic relationship of $\varphi(t)$ and the pit depth of corrosion $P(t)$ was established by Li *et al*. (2009) based on the experimental results published on the references

$$\phi(t)=\begin{cases}1.0 & p(t)<1.3mm\\ -0.79\,p(t)^2+1.88\,p(t)-0.10 & p(t)\geq 1.3mm\end{cases} \tag{31}$$

where $p(t)$ is the pit depth of corrosion, which is correlated to the service life and is calculated by Eq. (19).

The fatigue reliability index β can be derived based on the function $g(\boldsymbol{X})$ assuming that all random variables (i.e., A, ϕ, Δ, and S_{re}) are Lognormal as follows

$$\beta=\frac{\lambda_\Delta+\lambda_A+\lambda_\phi-(m\cdot\lambda_{S_{re}}+\ln n_{tc})}{\sqrt{\zeta_\Delta^2+\zeta_A^2+\zeta_\phi^2+\left(m\cdot\zeta_{S_{re}}\right)^2}} \tag{32}$$

where λ_Δ, λ_A, λ_ϕ, $\lambda_{S_{re}}$ and ζ_Δ, ζ_A, ζ_ϕ, $\zeta_{S_{re}}$ denote the mean value and standard deviation of ln(Δ), ln(A), ln(ϕ), and ln(S_{re}), respectively.

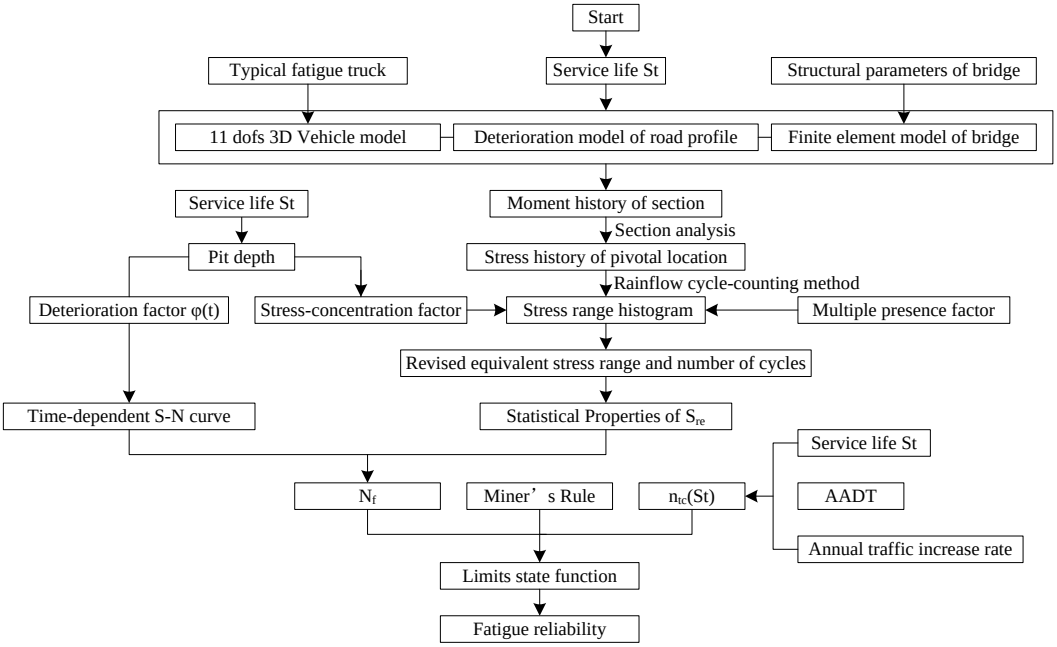

Fig. 2 Flowchart of the proposed framework of fatigue reliability evaluation

4.2 Target reliability index

The target reliability index β_T is defined as the value of reliability index that is acceptable for design or evaluation, and its selection should also be based on economic considerations, involving cost of construction, inspection, repair, rehabilitation, and replacement. In the present practice, this value can be applied as a standard against which one might measure safety of the bridge from the point of view of fatigue failure that initiates at a specified detail on the bridge.

To determine appropriate reliability index for a structure, target reliability indices according to purpose of structure have been developed. AASHTO LRFD prescribed the design criteria based on the target reliability index 3.5 (AASHTO 2007). Joint Committee of Structural Safety (Diamantidis 2001, Ractwitz 2000) and European Committee for Standardization (CEN 2002) also have proposed target reliability indices according to the purpose and condition of structures. These indices are classified in accordance with consequences of failure and relative cost of safety measure. The target reliability indices were ranged from 1.54 to 6.0 according to previous studies.

In this study, the main structure is composed by six girders and therefore has low degrees of redundancy. A fatigue collapse of the structure after the breaking of the first reinforcing steel or prestressing tendon of one of the girders is therefore expected. According to AASHTO LRFD code, a value of 3.5 is adopted in this study. It is worth pointing out that the target level of 3.5 is selected as a relative norm in the AASHTO LRFD code calibration process as the average of levels instead of an absolute criterion.

4.3 Framework of fatigue reliability prediction of PSC highway bridges

The proposed procedure for the fatigue reliability evaluation of PSC highway bridges (as

shown in Fig. 2) is summarized as following:

Step 1: investigate the details of structural members; determine ADTT, annual traffic increase rate, and service life;

Step 2: build the finite element model of bridge and fatigue truck model; determine road surface condition according to the present service life; conduct the vehicle-bridge coupled vibration analysis under single fatigue truck, gain maximum moment range and the number of cycle under one passage of a fatigue truck;

Step 3: determine stress history of concrete, reinforce steel and prestressing tendons in critical location by sectional analysis;

Step 4: determine the stress-concentration factor of steel bar and prestressing tendons;

Step 5: determine multiple presence factor of vehicle according to span length, ADTT, and number of lanes;

Step 6: determine the stress range spectrum chart according to rain-flow counting method;

Step 7: determine stress range cut-off levels to estimate the equivalent stress range and stress cycles per one truck passage;

Step 8: determine time-dependent S-N curve according to the service life and Eq. (31);

Step 9: construct the fatigue limit stated function according to Miner's rule, S-N curve and the total number of stress cycles in entire service life;

Step 10: perform fatigue reliability analysis by Monte Carlo simulation or simplified method, such as Eq. (32).

5. Application example to a PSC bridge

To demonstrate the effectiveness of the proposed procedure, fatigue reliability analysis of a short span six-girder PSC simple supported bridge designed in accordance with Chinese bridge design specifications is presented in this study.

5.1 Structural configuration

The simply supported PSC bridge considered herein is located in the Tianjin Binhai New Area of China, and has been in service from June 2011. The bridge has a span length of 30 m and three-lane-roadway in the same direction with the total width of 13.5 m. The cross section of the bridge is shown in Fig. 3. The distance from the center of each adjacent T-type girder is 2.25 m. The bridge was designed according to the China Code (JGJ D62-2004) for a Highway-I live load. There are a 150 mm thick reinforced concrete slab and 100 mm asphalt concrete overlay. Reinforcing steel is 335 MPa, the ultimate strength of the prestressing tendons is 1860 MPa and there is a 50 mm thick concrete cover. The total area of the prestressing tendons in the mid-span section of the girder G3 is 4200 mm^2 and the distribution of the prestressing tendons in the same section is shown in Fig. 4.

The average daily truck traffic (ADTT) at the early stage after it is open to the public is about 3000 vehicle/day with 60% in the right lane, 30% in the center lane and 10% in the left lane. The service life of the bridge is taken as 100 years. The bridge is located within 2 km of the coast and is exposed to repeated use of deicing salts during the winter seasons. A relative humidity of 70% is used for the predictive model for corrosion rate.

The multi-girder bridge is treated as a grillage beam system (shown in Fig. 5), and is modeled

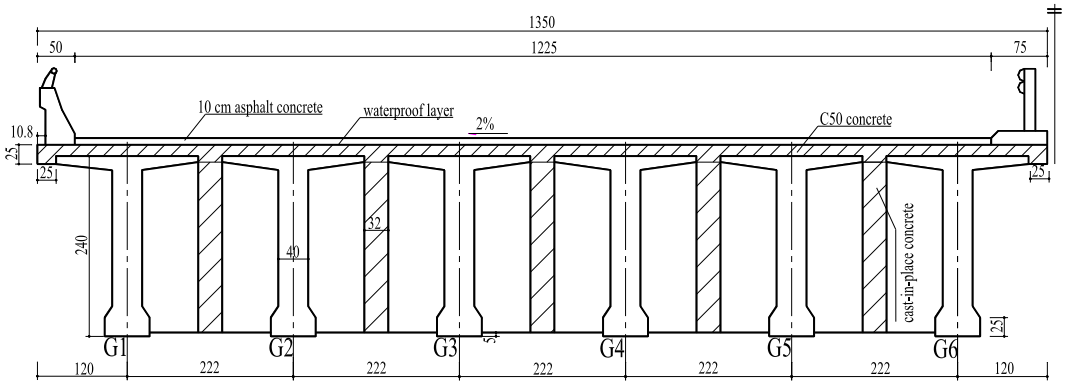

Fig. 3 Configuration of the bridge in the mid-span section (units: cm)

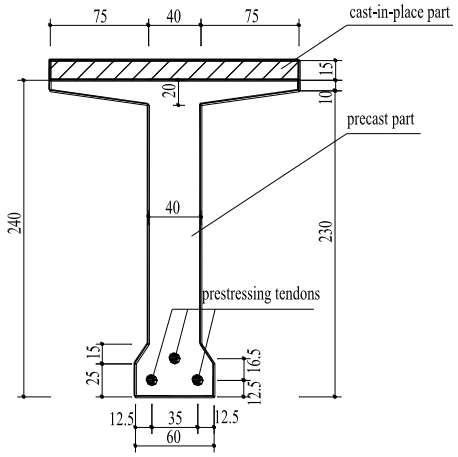

Fig. 4 Prestressing tendons in the mid-span section of Girder G3 (units: cm)

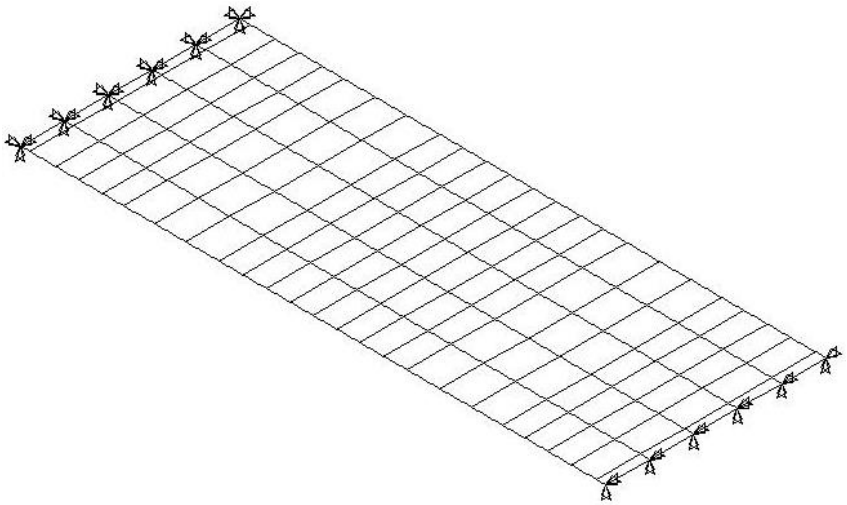

Fig. 5 The grillage beam system

Table 2 Probabilistic models of the variables used in the example

Variable	Distribution	Mean	COV	Source
A	Lognormal	1.58×10^{24}	0.15	(Li *et al*.2009)
m	Constant	3	-	(Li *et al.* 2009; Byers *et al*. 1997)
$AADT$	Normal	3000	0.2	
κ	Normal (truncated by 1)	Calculated by Eq.(5)	0.35	
$\varphi(\cdot)$	Lognormal	Calculated by Eq.(13)	0.2	
Δ	Lognormal	1	0.15	(Kwon and Frangopol 2010)

Table 3 Parameters selected for parametric study

Parameters	Variation
Overload factor	1.0,1.5,1.8,2.0, 3.0
Vehicle speed (km/h)	20, 40,60,100,120
Annual traffic increase rate (%)	0,2,5,10
Maintenance interval of road surface (years)	5,10,15

using the ANSYS parametric design language capabilities-APDL language. The bridge is analyzed by finite element method using 1925 BEAM4 elements of equal lengths and 300 equal time steps for different velocities. The time step is set as $\Delta t=L/v$ and $\Delta t<1/(10f)$, in seconds, where f=4.121 Hz is the basic frequency of the bridge; v is the speed of vehicle, in m/s; L is the length of element, 0.1 m is arbitrarily set in the present study. For a demonstrational purpose, the typical girders of G1, G2 and G3 are selected for fatigue reliability analysis in the present study.

5.2 Fatigue reliability prediction

The fatigue life of the prestressed concrete girder is controlled by the worst prestressing tendon and the fatigue life of prestressing tendon is controlled by stress range of the tendon. The stress range pertaining to the number of load cycle is therefore taken as primary parameter. The probabilistic model parameters for the variables are listed in Table 2.

A number of factors affect the fatigue reliability of the concerned bridge during the service cycle subjected to moving highway vehicle such as the overload factor, the vehicle speed, the annual traffic increase rate, the road profiles etc. In order to better understand the influence of these factors, a parametric study is performed following the proposed procedure. Table 3 lists different parameters selected for the parametric study. Only one variable is changed at a time to assess its individual effect. The detailed results are provided in the following subsections.

5.2.1 Influence of overload factor

Overload factor λ_L is characterized by over-weight level relative to the axle load of fatigue truck. Five overload cases with the factors λ_L of 1.0, 1.5, 1.8, 2.0 and 3.0 are considered in the present analysis. It should be noted that the factors λ_L in Table 3 are determined according to the survey on traffic trucks and recent failures of highway bridges in China. The survey indicates that λ_L of 1.8 is very common in China, and part of highway bridges are subjected to λ_L of 2.0. The cases of λ_L=3.0 represents the extreme overload condition, which frequently results in bridge abrupt collapse.

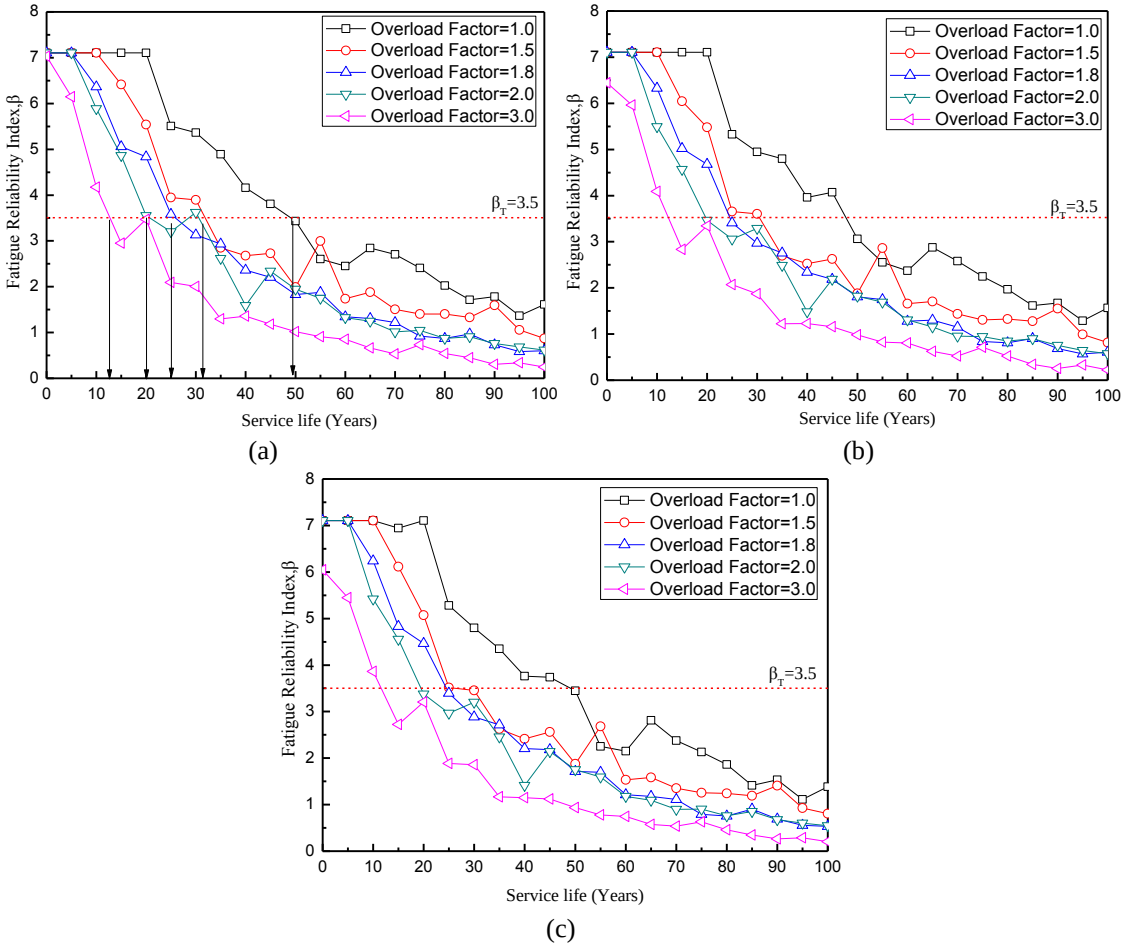

Fig. 6 Fatigue reliability profiles of the bridge in different overload factors (a) Girder G1, (b) Girder G2, and (c) Girder G3

In order to evaluate the influence of the overload factor on the fatigue performance of the prototype bridge, the reliability indices β at different stages in the life span are calculated at the vehicle speed of 40 km/h, the traffic increase rate of 0.02 and the road surface maintenance interval of 10 years. The results are shown in Fig. 6. As expected, the reliability index β for fatigue damage decreases dramatically with the increase in the service life, and the profile declines more sharp for larger overload factor.

If the target reliability index is predefined as β_T=3.5, the first exceed life of girder G1 can be evaluated as 49.5, 31.5, 25, 20 and 12.8 years at the overload factor of 1.0, 1.5, 1.8, 2.0 and 3.0, respectively. The relationship between the first exceed time of fatigue reliability and the overload factor is plotted in Fig. 7. It can be observed that the service life decreases dramatically with the increase of the overload factor. The overload factor increases from 1.0 to 1.8, corresponding to the common case in China, the deterioration of bridge due to corrosion-fatigue action will be accelerated, and the service life of the bridge will be a half of the original design life.

To investigate the lateral distribution effect of the vehicles on the multiple lanes, the fatigue

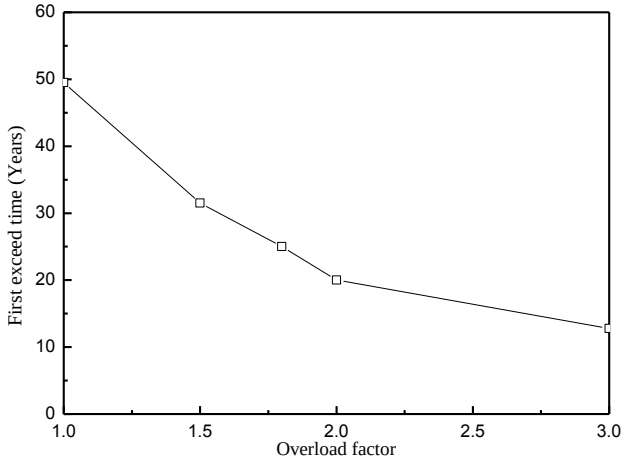

Fig. 7 First exceed times of fatigue reliability vs. the overload factors for girder G1

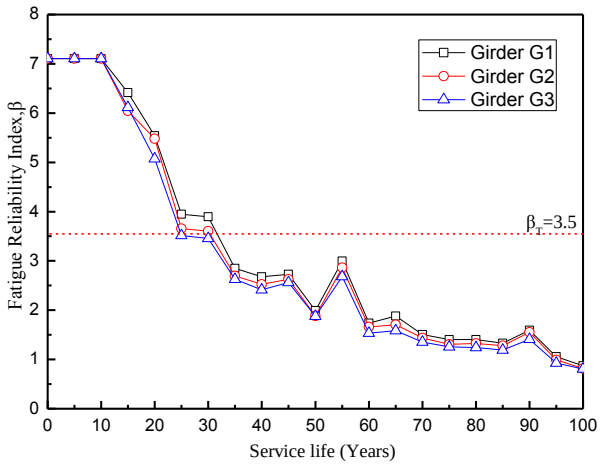

Fig. 8 Fatigue reliability profiles of the bridge of different girders

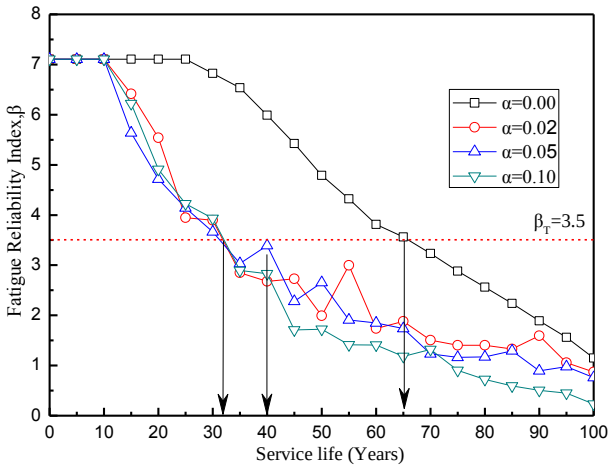

Fig. 9 Fatigue reliability profiles of the girder G1 in different traffic increase rates

reliability profiles of three girders of G1, G2 and G3 for the overload factor of 1.5 are shown in Fig. 8. It can be seen from Fig. 8 that the girder G1 is only a little later than G2 and G3. In sum, in the case of the distribution of the vehicle on the lanes in the present example, there is little difference displays between the three girders of G1, G2 and G3.

5.2.2 Influence of traffic increase rate

To evaluate the fatigue life, AADT is an important variable which directly affects the specific traffic loads on the bridge. AADT varies over years and is influenced by numerous factors like local birth rate and local gross domestic product (GDP). Local traffic departments often adopt an increase rate (α) to predict future traffic flow, which is typically calculated using Eq. (8) (Sliupas 2006)

$$\alpha = \sqrt[k]{\frac{E_t}{E_{t-k}}} - 1 \tag{33}$$

where k is the number of the total years in which AADT data is available, t is the most recent year with the available AADT data, E_t denotes the AADT of the t^{th} year, and E_{t-k} denotes the AADT of the $(t-k)^{\text{th}}$ year.

The effect of AADT on the fatigue reliability is studied by changing the annual traffic increase rate α from 0.0 to 0.10. This study is conducted for an overload factor of 1.5, the vehicle speed of 40 km/h and the road surface maintenance interval of 10 years. The results calculated for the girder G1 are presented in Fig. 9. It is observed that if the AADT maintains original level in the present study, the service life will reach more than 65 years corresponding to the target reliability index of 3.5. However, if the annual traffic increase rate range from 0.02 to 0.10, the fatigue reliability profiles changed sharply, the first time exceeds the target reliability index is at about 32 years. The difference between three traffic increase rates is negligible.

5.2.3 Influence of vehicle speed

As stated earlier by many researchers, the vehicle speed has ambiguous effect on the impact factor of multi-girder bridge. Resonance will occur when the vehicle passes the bridge at a specific speed. In the present study, there is not obvious discrepancy of fatigue reliability of the girder G1 for the five different vehicle speeds as shown in Fig. 10. Similar results can also be observed for the girder G2 and G3, which are not presented herein. The fatigue reliability is unaffected by vehicle speed for the PSC bridge selected for study.

5.2.4 Influence of deck surface maintenance interval

The deck surface suffers from the wheels of vehicle directly, which induces its deterioration during the service stage of the bridge. The AASHTO C4.7.2.1 also indicates that the deck surface roughness is a major factor in vehicle/bridge interaction and it is difficult to estimate the long-term deck deterioration effects thereof at the bridge design stage. As stated earlier, in order to improve the deck surface roughness, the maintenance actions for refitting the deck surface are generally performed every 15 years. But the maintenance interval of deck surface may be adjusted to 5 or 10 years according to the practical deterioration status of deck surface.

To evaluate the effect of the deck surface maintenance interval on fatigue reliability of the bridge, the deck surface maintenance interval of 5, 10 and 15 years are considered at an overload factor of 1.5, a vehicle speed of 40 km/h and the traffic increase rate of 0.02. Fig. 11 presents the

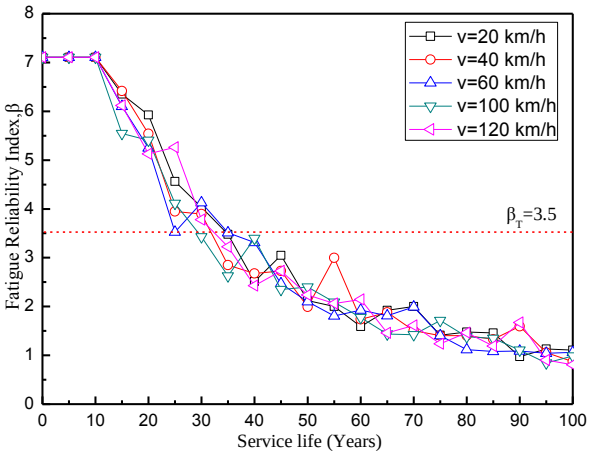

Fig. 10 Fatigue reliability profiles of the girder G1 in different vehicle speeds

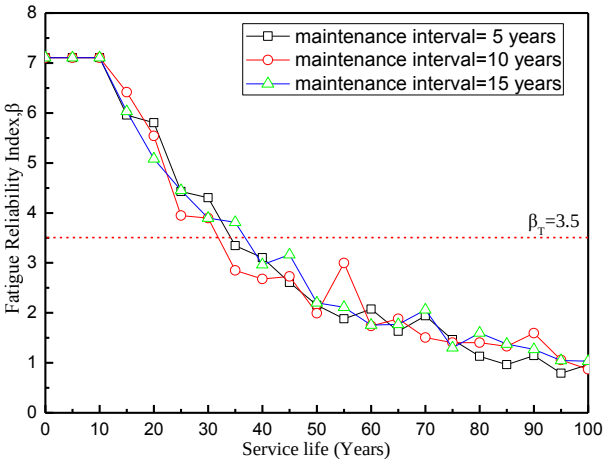

Fig. 11 Fatigue reliability profiles of the girder G1 at different road surface maintenance interval

relation of fatigue reliability profiles of the girder G1 at different road surface maintenance interval. It can be seen that the deck surface maintenance interval has no distinct effect on the fatigue reliability profiles. So in practice the deck surface should be retrofitted for the driving conditions, not based on the safety.

5.3 Discussions

As indicated earlier, PSC highway bridges are traditionally immune to fatigue damage. Up to now, fatigue failure of PSC highway bridges is neglected by most of design specifications. However, in many developing countries, more and more overloaded trucks increase the potential fatigue failure risk of highway bridges.

Results from the parametric study can be summarized and the following observations are made within the context of fatigue reliability of PSC highway bridges defined in this paper. The overload factor and the annual traffic increase rate are the primary parameters that affect the fatigue

reliability significantly. The vehicle speed and the deck surface maintenance interval however have minor influence. It is worth noting that the conclusions are drawn under the specific assumptions for the bridge used for demonstration. The results and the conclusions may be different if the assumptions are different. The proposed method framework is suitable for fatigue reliability prediction of new and existed PSC bridges in any predefined conditions. This framework is of significant use for bridge designers.

6. Conclusions

This paper presents a comprehensive framework for fatigue reliability prediction of PSC highway bridges under fatigue loads due to vehicles in erosive environment. The vehicle-bridge coupling vibration analysis is utilized as the tool for obtaining the stress history of concerned prestressing tendons considering the dynamic impact effects automatically. The stress-concentration factor of steel bars or prestressing tendons is derived by the consideration of corrosion pit depths. As an illustrative example, a short span six-girder PSC simple supported bridge is analyzed, and some conclusions are drawn:

(1) The overload factor increases from 1.0 to 1.8, the deterioration of bridge due to corrosion-fatigue action will be accelerated, and the service life of the bridge will become a half of the original design life.

(2) The increase of traffic volume affects the fatigue reliability profiles significantly, the first time exceeds the target reliability index will be brought forward from 65 years to 32 years when the annual traffic increase rate varies from 0.02 to 0.10. The difference between three traffic increase rates is indistinctive.

(3) The fatigue reliability is unaffected distinctly by vehicle speed and deck surface maintenance interval.

(4) As studied in this paper, the S-N curves of steel bars and prestressing tendons are deteriorating in the service stage due to the corrosion, but the bond slip between concrete and steel is neglected, which should be further investigated in the future study.

(5) Finally, it was observed that if the target reliability index is less than 3.5, the predicted service life will be increased sharply. A rational predefined target reliability index of the component or the system may influence the results and should also be focused on in the future study.

Acknowledgments

This work reported here was supported by the National Science Fund of China (51178305) and the Key Projects in the Science & Technology Pillar Program of Tianjin (11ZCKFSF00300). Any opinions, findings and conclusions or recommendations expressed in this paper are those of the authors and do not necessarily reflect those of the sponsor.

Reference

AASHTO (2007), AASHTO LRFD Bridge Design Specification,s 4th Edition, American Association of

State Highway and Transportation Officials, Washington, DC.
Al-Hammoud, R., Soudki, K. and Topper, T.H. (2011), "Fatigue flexural behavior of corroded reinforced concrete beams repaired with CFRP sheets", *J. Compos. Constr.*, **15**(1), 42-51.
Au, F.T.K., Cheng, Y.S. and Cheung, Y.K. (2001), "Effects of random road surface roughness and long-term deflection of prestressed concrete girder and cable-stayed bridges on impact due to moving vehicles", *Comput. Struct.*, **79**(8), 853-872.
Byers, W.G., Marley, J.M., Mohammad, J. and Sarkani, S. (1997), "Fatigue reliability reassessment procedures: state-of-the-art paper", *J. Struct. Eng.*, **123**(3), 271-276.
Bowman, M.D., Fu, G.K., Zhou, W.E., Connor, R.J. and Godbole, A.A. (2012), *Fatigue Evaluation of Steel Bridges (NCHRP 721)*, Transportation Research Board, Washington, D.C.
Casas J.R. (1999), "Safety of partially prestressed highway bridges", *IABSE Struct. Eng. Int.*, **9**(3), 206-211.
CEN (2002), "Eurocode 0: basis of structural design", The European Standard EN1990, European Committee for Standardization.
Cesar, C.M. and Joan, R.C. (1998), "Fatigue reliability analysis of prestressed concrete bridges", *J. Struct. Eng.*, **124**(12), 1458-1466.
Collins, M. and Mitchell, D. (1987), *Prestressed concrete basics*, 1st Edition, Canadian Prestressed Concrete Institute, Ottawa, Ont.
Diamantidis, D. *et al.* (2001), *Probabilistic assessment of existing structures*, Joint Committee on Structural Safety (JCSS), RILEM Publications.
Emilio, B.A., Philippe, B., Alaa, C. and Mauricio, S.S. (2009), "Probabilistic lifetime assessment of RC structures under coupled corrosion-fatigue deterioration processes", *Struct. Saf.*, **31**(1), 84-96.
Guo, T. and Chen, Y.W. (2011), "Field stress/displacement monitoring and fatigue reliability assessment of retrofitted steel bridge details", *Eng. Fail. Anal.*, **18**(1), 354-363.
Honda, H., Kajikawa, Y. and Kobori, T. (1982), "Spectra of road surface roughness on bridges", *J. Struct. Div.*, **108**(9), 1956-1966.
Huang, D.Z., Wang, T.L. and Shahawy, M. (1993), "Impact studies of multigirder concrete bridges", *J. Struct. Eng.*, **119**(8), 2387-2402.
ISO 8608(1995), Mechanical vibration-Road surface profiles Reporting of measured data, *ISO*.
Joan, R.C. and Cesar, C.M. (1998), "Probabilistic response of prestressed concrete bridges to fatigue", *Eng. Struct.*, **20**(11), 940-947.
Kwon, K. and Frangopol, D.M. (2010), "Bridge fatigue reliability assessment using probability density functions of equivalent stress range based on field monitoring data", *Int. J. Fatigue*, **32**(8), 1221-1232.
Leitão, F.N., da Silva, J.G.S., da S. Vellasco, P.C.G., de Andrade, S.A.L. and de Lima, L.R.O. (2011), "Composite (steel-concrete) highway bridge fatigue assessment", *J. Constr. Steel Res.*, **67**(1), 14-24.
Li, X.X., Wang, Z.X. and Ren, W.X. (2009), "Time-dependent reliability assessment of reinforced concrete bridge under fatigue loadings", *China Railw. Sci.*, **30**(2), 49-53. (in Chinese)
Miner, M.A. (1945), "Cumulative damage in fatigue", *Trans. ASME., J. Appl. Mech.*, **67**, A159-A164.
Petryna, Y.S., Pfanner, D., Stangenberg, F. and Krätzig, W.B. (2002), "Reliability of reinforced concrete structures under fatigue", *Reliab. Eng. Syst. Saf.*, **77**(3), 253-261.
Pipinato, A. and Modena, C. (2010), "Structural analysis and fatigue reliability assessment of the Paderno bridge", *Pract. Period. Struct. Des. Constr.*, **15**(2), 109-124.
Rackwitz, R. (2000), "Optimization-the basis of code-making and reliability verification", *Struct. Safe.*, **22**(1), 27-60.
Rigon, C. and Thürlimann, B. (1985), "Fatigue tests onpost-tensioned concrete beams", *Institut fur Baustatik und Konstruktion Eidgenossische Technische Hochschule*, Zurich, Switzerland.
Šliupas, T. (2006), "Annual average daily traffic forecasting using different techniques", *Transport*, **21**(1), 38-43.
Stangenberg, F. *et al.* (2009), *Lifetime-oriented Structural Design Concepts*, Springer, Berlin.
Taly, N. (1989), *Design of modern highway bridges*, McGraw-Hill Book Companies, Inc., New York.
Vu, K.A.T. and Stewart, M.G. (2000), "Structural reliability of concrete bridges including improved chloride-induced corrosion models", *Struct. Safe.*, **22**(4), 313-333.

Wang, T. L., Huang, D.Z. and Shahaway, M. (1992), "Dynamic response of multigirder bridges", *J. Struct. Eng.*, **118**(8), 2222-2238.

Warner, R.F. and Hulsbos, C.L. (1966), "Probable fatigue life of prestressed concrete beams", *J. Prestres. Concrete Inst.*, **11**(2), 16-39.

Wu, J., Chen, S.R. and John, W. van de L. (2012), "Fatigue assessment of slender long-span bridges: reliability approach", *J. Bridge Eng.*, **17**(1), 47-57.

Zhang, W. and Cai, C.S. (2012), "Fatigue reliability assessment for existing bridges considering vehicle speed and road surface conditions", *J. Bridge Eng.*, **17**(3), 443-453.

Zhu, J.S. and Yi, Q. (2013), "Bridge-vehicle coupled vibration response and static test data based damage identification of highway bridges", *Struct. Eng. Mech.*, **46**(1), 75-90.